4. H. CHANG and S. SASTRI, *Met. Trans.* 8A (1977) 1063.
5. R. RAY, Patent pending assigned to Allied Chemical Corporation, Morristown NJ, USA, and *J. Mater. Sci.* 16 (1981) 2924.
6. M. R. GLICKSTEIN, R. J. PATTERSON II and N. E. SHOCKEY, "Rapid Solidification Processing", edited by R. Mehrabian, B. H. Kear and M. Cohen (Claitor's Publishing Division, Baton Rouge, Louisiana, 1978).
7. N. J. GRANT, "Rapid Solidification Processing", edited by R. Mehrabian, B. H. Kear and M. Cohen (Claitor's Publishing Division, Baton Rouge, Louisiana, 1978).

Received 10 April
and accepted 15 May 1981

RANJAN RAY
Marko Materials Inc.,
P.O. Box 3,
North Billerica, MA 01862,
USA

The preparation and characteristics of ZrC and TaC single crystals using an r.f. floating-zone process

TaC exhibiting superconductivity has the highest melting point (~ 3900° C) of the refractory carbides, hence, its single crystal has not been obtained using the radio frequency (r.f.) floating-zone process [1]. In contrast, the authors have grown comparatively large single crystals of TaC by the r.f. floating-zone process. Prior to growing TaC crystals the preparation of ZrC single crystals was attempted. The method of preparation was based on the knowledge that single crystals of NbC with nearly the same melting point at ZrC, have previously been grown using an r.f. generator of 30 kW [2], but it was impossible to obtain ZrC single crystals using this method. By contrast, an r.f. generator of 50 kW made it possible to grow large ZrC single crystals easily. The present note describes the preparation and characteristics of ZrC and TaC single crystals grown by the r.f. floating-zone process at a pressure of 10 atm.

The operating procedures for growing crystals were essentially the same as those previously described for TiC [3] and NbC [2]. The working coil for ZrC was a six- or eight-turn co-planar coil of water-cooled copper tubing, while for TaC an eight-turn co-planar coil was used. The growth of TaC single crystals is far more difficult than ZrC. About 1 h after the formation of the molten zone of TaC, the crack initiated at the surface of the specimen, but it was possible to observe the molten material through the crack. The fundamental difficulties in growing TaC single crystals result from the surface tension not being sufficiently high to maintain a zone with a high density (14.5 g cm^{-3}). Also the coils are punctured by arcing between the coil and melt.

Metallic-looking ZrC single crystals 8 mm in diameter and 60 mm long were grown. A typical example is shown in Fig. 1. Fig. 2 shows the TaC single crystal appearing at the cleavage planes. Except for the surface of the crystal, which was a golden yellow colour, it had a silver metallic look. There was a longitudinal crack. The macrophotographic observation of the cross-section along the dotted line in Fig. 2a is shown in Fig. 2b. There appears to be a large melted grain and a cleavaged crack. ZrC was greater than 99.9% pure and TaC was 99.5% pure as determined by X-ray fluorescence analysis. The average chemical composition was $ZrC_{0.9}$ and $TaC_{0.83}$ as obtained by chemical analysis and electron microprobe X-ray analysis. X-ray powder diffraction patterns of crushed specimens indicate a lattice parameter of $a_0 = 0.4702$ and 0.4429 nm for ZrC and TaC, respectively. The growth direction almost coincided with the ⟨110⟩ or ⟨100⟩ direction in ZrC and the ⟨110⟩ direction in TaC. Dislocation pits of ZrC

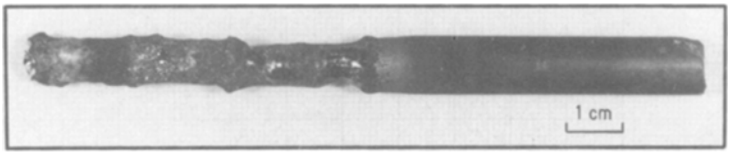

Figure 1 As-grown single crystal of ZrC.

0022–2461/81/102930–04$02.40/0

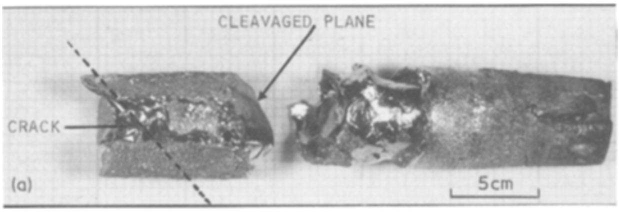

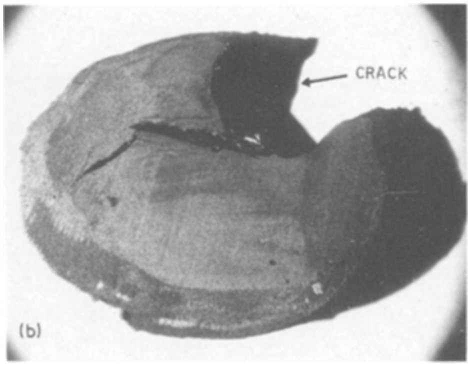

Figure 2 (a) As-grown single crystal of TaC. The cleavage plane is observed and the crack extends longitudinally and (b) the cross-section of the crystal along the dotted line in (a).

and TaC cleaved planes are shown in Fig. 3. The crystal quality of ZrC is better than that obtained by Lee and Haggerty [4] which were characterized by low-angle grain boundaries. The slip traces in TaC could be caused by thermal stress during crystal growth [2].

The C/Zr and C/Ta ratios determined by electron microprobe X-ray analysis along the growth and radial directions indicate that the C/Ta ratio has a slight scatter, but that the C/Zr ratio is almost constant.

The electrical resistance values of TaC single crystal, i.e. the golden yellow surface (1) and the inner part of the crystal (2) are shown in Fig. 4 at low temperatures. Both (1) and (2) become superconductors with the onset temperatures 9.0 and 7.15 K, respectively. The C/Ta ratio of the surface of the crystal (1) has a higher value than inner part of the crystal (2) so that the onset temperature of the former is higher than the latter when considering that TaC exhibits a decrease in the superconducting critical temperature with the departure from the stoichiometry [5]. The stepped change in Region (2) would be due to local fluctuation in the composition.

The periodicity of the hardness curves of ZrC and TaC, i.e. the four-fold symmetry in the (1 1 0) planes, is shown in Fig. 5. The present anisotropy and theoretical curves [6] indicate that the primary slip system of TaC is $\{1\,1\,1\}\langle 1\,\bar{1}\,0\rangle$, while in ZrC the $\{1\,1\,0\}\langle 1\,\bar{1}\,0\rangle$ system is found. This is consistent with previous works [6, 7]. The degree of anisotropy in the hardness [8] is 6.8% for ZrC and 2.0% for TaC. The former is comparable to the data of Hannink *et al.* [6]. A small anisotropy in TaC would firstly be due to the non-stoichiometry of the crystal and secondly due to the crystal quality such as high dislocation

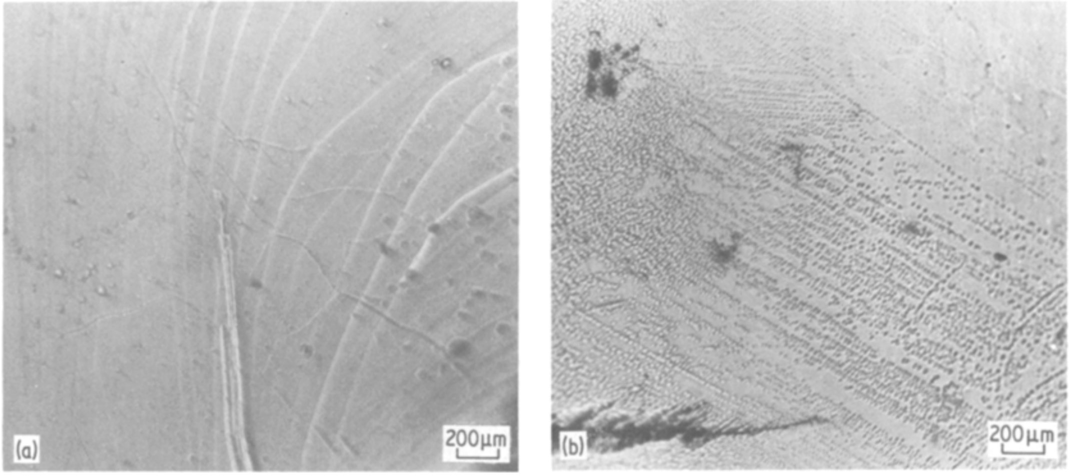

Figure 3 Etching patterns of (1 0 0) planes of (a) ZrC and (b) TaC single crystals.

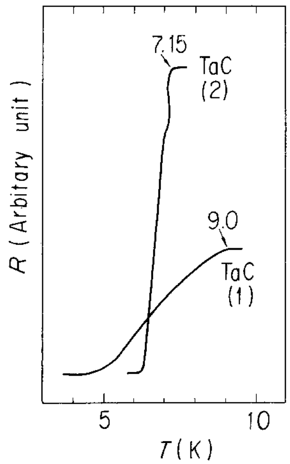

Figure 4 The low-temperature behaviour of the electrical resistance, R, of TaC single crystals: (1) Golden yellow surface of the crystal and (2) inner part of the crystal.

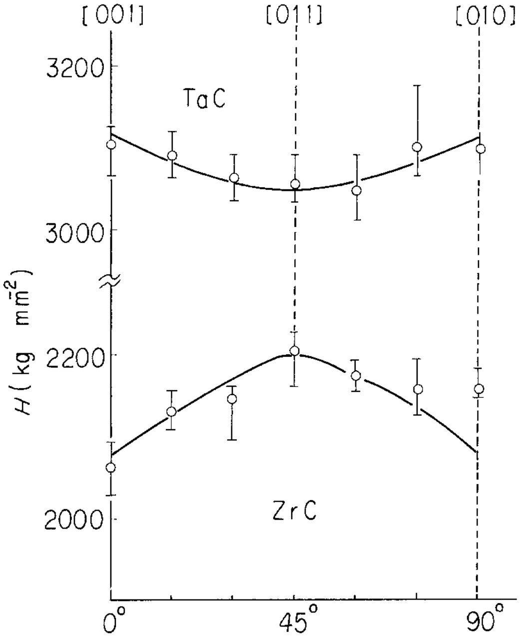

Figure 5 Vickers microhardness anisotropy of ZrC and TaC (1 0 0) planes.

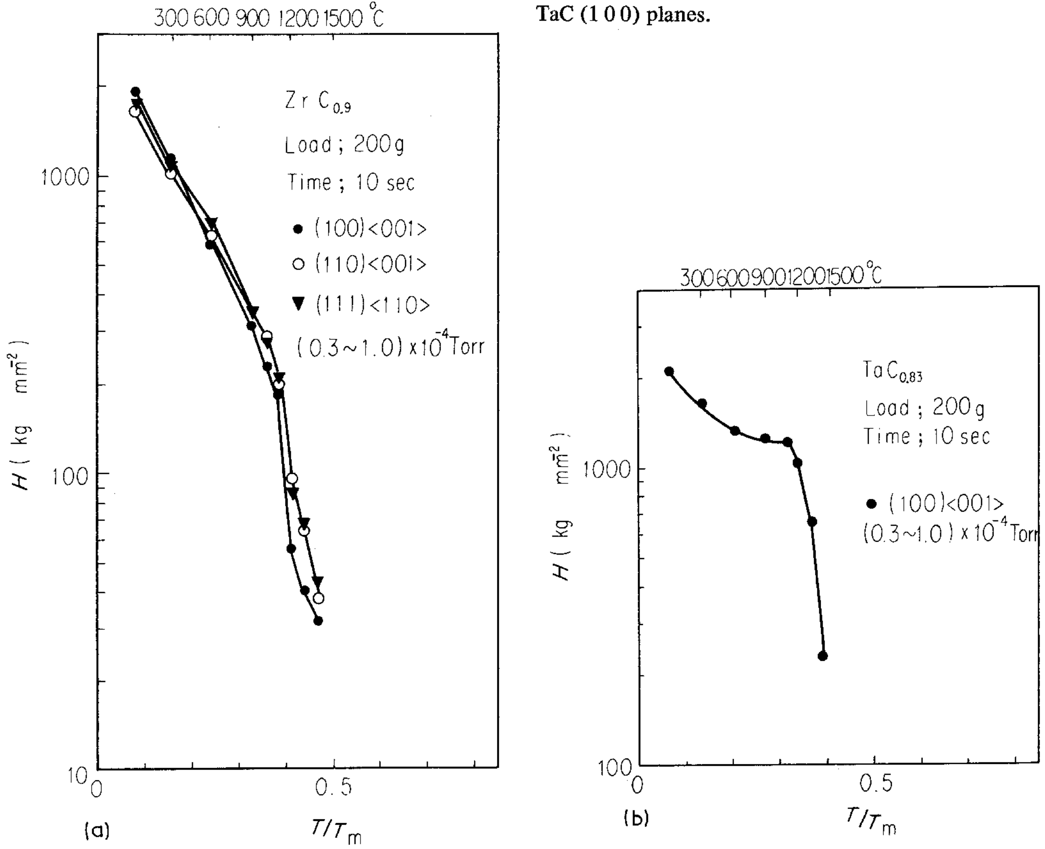

Figure 6 A logarithmic plot of hardness against homologous temperature. T_m represents the melting point: (a) $ZrC_{0.9}$ and (b) $TaC_{0.83}$.

density. In fact, $TaC_{0.96}$ single crystals grown by the flux method [7] show a larger anisotropy than those grown by the method here, and $TiC_{1.0}$ single crystals with a low dislocation density of 10^3 cm^{-2} indicate pronounced anisotropy in the hardness [8].

High-temperature indentation was performed using the Nikon high-temperature micro-hardness tester model QM [8, 9]. Cracks observed at each corner at room temperature diminish at 900 and 1200° C in $ZrC_{0.9}$ and $TaC_{0.83}$, respectively. This is explained in terms of the dislocation mobility corresponding to the kneek in a logarithmic plot of hardness against homologous temperature T/T_m represented in Fig. 6. The gradual decrease in the hardness of $TaC_{0.83}$ up to a temperature of 1100° C is characteristic, while in the case of $ZrC_{0.9}$ a drop in hardness of about × 10 occurs in the same temperature range. The temperature dependence of hardness in $TaC_{0.83}$ is similar to that in another fcc metal (Cu) and co-valent semiconductors (Si and Ge) [6] with the $\{1\,1\,1\}\langle 1\,\bar{1}\,0\rangle$ slip system.

Acknowledgements

The authors whish to acknowledge the very valuable contribution of Dr K. Kaneko to the chemical analysis of the crystals. They also express thanks to Dr Y. Okada for the macro-photograph.

References

1. M. B. PACKER and M. J. MURRAY, *J. Cryst. Growth* **16** (1972) 240.
2. Y. KUMASHIRO, E. SAKUMA, Y. KIMURA, H. IHARA and S. MISAWA, *J. Less-Common Met.* **75** (1980) 187.
3. Y. KUMASHIRO, A. ITOH and S. MISAWA, *ibid.* **32** (1973) 21.
4. D. W. LEE and J. S. HAGGERTY, *J. Amer. Ceram. Soc.* **52** (1969) 641.
5. L. E. TOTH, "Transition Metal Carbides and Nitrides" (Academic Press, New York, 1971) p. 215.
6. R. H. HANNINK, D. L. KOHLSTEDT and M. J. MURRAY, *Proc. Roy. Soc. Lond.* **A326** (1972) 406.
7. D. J. ROWCLIFFE and G. E. HOLLOX, *J. Mater. Sci.* **6** (1971) 1270.
8. Y. KUMASHIRO, A. ITOH, T. KINOSHITA and M. SOBAJIMA, *ibid.* **12** (1977) 595.
9. Y. KUMASHIRO and E. SAKUMA, *ibid.* **15** (1980) 1321.

Received 2 December 1980
and accepted 2 March 1981

Y. KUMASHIRO
Electrochemical Laboratory,
1-1-4, Umezono,
Sakura-mura,
Niihari-gun,
Ibaraki 305,
Japan
Y. NAGAI
H. KATŌ
Nippon Kogaku K. K. Research Laboratory,
1-6-3 Nishi-ohi,
Shinagawa-ku,
Tokyo 140,
Japan
E. SAKUMA
K. WATANABE
S. MISAWA
Electrochemical Laboratory,
1-1-4, Umezono,
Sakura-mura,
Niihari-gun,
Ibaraki 305,
Japan